The reservoir network: A new network topology for district heating and cooling

Tobias Sommer[1], Matthias Sulzer[2], Michael Wetter[3], Artem Sotnikov[1], Stefan Mennel[1], Christoph Stettler[1]

[1]Institute of Building Technology and Energy, Lucerne University of Applied Sciences and Arts, CH 6048 Horw, Switzerland

[2]Empa, Swiss Federal Laboratories for Materials Science and Technology, CH 8600 Dübendorf, Switzerland

[3]Building Technology and Urban Systems Division, Lawrence Berkeley National Laboratory, 1 Cyclotron Road, Berkeley, CA 94720, USA

[*]Corresponding author: T. Sommer, tobias.sommer@hslu.ch

1. Abstract

Thermal district networks are effective solutions to substitute fossil fuels with renewable energy sources for heating and cooling. Moreover, thermal networking of buildings allows energy efficiency to be further increased. The waste heat from cooling can be reused for heating in thermal district systems. Because of bidirectional energy flows between prosumers, thermal networks require new hydraulic concepts. In this work, we present a novel network topology for simultaneous heating and cooling: the reservoir network. The reservoir network is robust in operation due to hydraulic decoupling of transfer stations, integrates heat sources and heat sinks at various temperature levels, and is flexible in terms of network expansion.

We used Modelica simulations to compare the new single-pipe reservoir network to a base-case double-pipe network, taking yearly demand profiles of different building types for heating and cooling. The electric energy consumed by the heat pumps and circulations pumps differs between the two networks by less than 1 %. However, if the reservoir network is operated with constant instead of variable mass flow rate, the total electrical consumption can increase by 48 % compared to the base case. As with any other network topology, the design and control of such networks is crucial to achieving energy efficient operation.

Investment costs for piping and trenching depend on the district layout and dimensioning of the network. If a ring layout is applied in a district, the reservoir network with its single-pipe configuration is more economical than other topologies. For a linear layout, the piping costs are slightly higher for the reservoir network than for the base case because of larger pipe diameters.

Key words: district heating networks; district cooling networks; Modelica; prosumer; reservoir network; piping costs

Published as: Tobias Sommer, Matthias Sulzer, Michael Wetter, Artem Sotnikov, Stefan Mennel and Christoph Stettler. The reservoir network: A new network topology for district heating and cooling. Energy, 199, 2020. https://doi.org/10.1016/j.energy.2020.117418

2. Introduction

District heating is an effective measure to reduce CO_2 emissions in urban areas and hence to limit global warming [1,2]. While global warming is already progressing, the cooling of buildings is becoming more relevant in urban energy systems [3–5]. As cooling produces waste heat that can be recovered and used for heating purposes, energy efficiency will be enhanced by integrating heating and cooling applications in holistic energy concepts [6,7]. In order to capture such efficiency potentials, buildings must be connected by thermal networks, allowing them to exchange their surplus energy.

Today, the focus in district heating development is on reducing network temperatures from close to 100 °C to below 70 °C. Such temperature reductions are described by the transition from the 3rd to the 4th generation of district heating systems [8]. The main benefits of the 4th generation of district heating (4GDH) systems are the reduction of thermal losses and the integration of low-temperature heat plants into the network [9]. Most 4GDH systems operate at network temperatures close to 60 °C to fulfil the requirements for space heating (supply temperatures of 35 °C to 60 °C in modern or retrofitted buildings) and domestic hot water (supply temperature of around 60 °C to minimize legionella growth). However, such networks cannot provide cooling for buildings.

With increasing cooling demand, the phasing-out of fossil fuels, and the limited availability of biomass, new thermal grids have emerged, mainly in Switzerland and Germany [10]. These new grids are used for both heating and cooling purpose and are often operated at temperatures close to ground temperature. Such networks may be called the "5th Generation District Heating and Cooling (5GDHC) Networks" [10]. In the following work we will use this expression[1]. In 5GDHC, combinations of heat pumps, chillers, and heat exchangers provide useful energy at the required temperature levels for space heating, domestic hot water and cooling. Such systems are economically attractive and reduce CO_2 emissions, if renewable heat at low temperature is available (e.g. lake, ground water, sewage water, waste heat from data centres or industry) and if the district contains predominantly new or retrofitted buildings [11,12]. Because of bidirectional energy flows between buildings, the network topology of a central heat producer and distributed heat consumers is no longer the most suitable solution. New concepts are needed where all customers of the network, so called thermal prosumers (in the following called simply prosumers), are allowed to extract heat from and/or supply heat to the network.

Seven 5GDHC networks in Switzerland are documented in detail [13]. The low-temperature sources of these networks are waste heat from laboratories and data centres, or environmental heat from geothermal plants, ground water and lakes. The large thermal potential of lakes [14] is currently exploited in 179 documented cases in Switzerland [15]. The network topologies of these thermal networks differ from case to case [13]. The conventional network (CN) topology with a central source, a main circulation pump and throttling valves at each transfer station is an option that is based on traditional district heating networks. Others use a network topology with distributed circulation pumps. These systems have increased thermal efficiency by minimizing mixing losses [16].

[1] Assuming that the classification of the district energy systems into 1st to 4th generations is based on their successive reduction of supplied exergy to the networks, as indicated by the network temperature reduction, the networks compared in this paper represent the next, 5th generation.

Such networks are bidirectional networks (BN) and they define the base case for the following comparisons (Fig. 1a). Examples for BN with distributed circulations pumps in Switzerland are ETH Zurich, Campus Hönggerberg [17,18], Suurstoffi district in Rotkreuz [19,20], and the Friesenberg network operated by the Familiengenossenschaft Zurich [21]. Recently, a bidirectional networks has also been realized at Medicon Village, Lund, Sweden [22]. The three Swiss networks are fairly new installations which commenced operation between 2012 and 2014. Initial experiences have been analysed and documented.

One major learning experience from Hönggerberg and Suurstoffi, as well as from model calculations by [23], is that pump-to-pump interactions present a control challenge in the BN. Problems occur in particular when prosumers of different sizes act in the same network. In this case, prosumers with large circulation pumps strongly affect the mass flow rate through prosumers with small circulation pumps. A decrease of mass flow rate through a heat pump may cause freezing damage. Reverse flow through prosumers with smaller circulation pumps may even occur [23]. A general increase of circulation pump speed of all prosumer pumps to ensure sufficient mass flow rate to avoid freezing may lead to cavitation at the suction side of circulation pumps, if the system pressure is not simultaneously increased [24]. Booster pumps compensating for pressure drops along network pipelines and in storages can be used as work-arounds to minimize pump-to-pump interactions [23]. For decentralized solar plants that supply heat to the network, similar problems have been described [25] and model predictive control has been suggested to stabilize flow and temperatures in the substations [26]. However, achieving stable and robust network control remains challenging, especially when controlling mass flow rates becomes even more demanding as existing networks are geographically extended.

Motivated by these challenges, we propose a new network topology which we call the reservoir network (RN) [27,28]. The hypothesis is as follows: A simpler hydraulic design at comparable energy efficiency eliminates the shortcomings of the previous designs and ensures robust operation and expandability. The research questions are: (i) What drives efficiency in a 5GDHC network? (ii) How and under what circumstances can the RN topology reduce investment costs? (iii) Why does the RN achieve a more robust operation and is more flexible in adapting to changes in supply and demand? To answer these questions, we compare the BN topology to the new RN topology. The comparison considers (i) the electric energy consumption of heat pumps and circulation pumps, (ii) investment costs based on trenching, pipe diameters and lengths and (iii) a qualitative discussion of the hydraulic design.

The paper is structured as follows: First, we explain the terminology of elements used in the BN and the RN topology. Thereafter, a general description of the BN and the RN topology is presented, which is followed by a description of the specific elements and their design criteria, boundary conditions, heating and cooling demands and control. Within this framework, simulations are carried out using the Modelica Buildings library [29] and the Dymola modeling and simulation environment for both the RN and the BN. Finally, the findings are summarized and limitations as well as opportunities of both topologies are discussed.

3. Terminology

A *thermal network* is a system of pipes filled with a fluid, typically water, as thermal energy carrier. Circulation pumps and valves control the mass flow rates in the network. The elements of the network which extract or supply thermal energy are called *agents*. Agents use heat exchangers to extract thermal energy from the network or supply thermal energy to the network, and are subdivided into *prosumers*, *plants* and *storages*, depending on their specific characteristics. We define the different agents as follows:

Prosumer: A prosumer is an agent whose main task is to cover the heating or cooling demand of buildings or processes. The term "prosumer" is a neologism formed by the words "producer" and "consumer", indicating that a prosumer can supply thermal energy to the network as well as extract thermal energy from it, depending on whether the prosumer has a net cooling or heating demand. Typical prosumers are buildings, data centres and industrial applications. For example, an office building is a prosumer with heating demand in winter and cooling demand in summer. A data centre is a prosumer with cooling demand only. The energy supplied to the network by a prosumer's cooling process is called waste heat.

Plant: A plant is an agent whose main task is to balance the net annual thermal energy demand of the prosumers. The plant itself has no demand, but instead provides a service to equalize the energy balance. This distinguishes the plant from the prosumer. The term "waste heat" in this paper is not used for plants, because waste heat is a product of cooling demand and is thus a characteristic of a prosumer. For example, in networks where the sum of all prosumers results in a net annual heating demand, a plant supplies thermal energy to the network in order to balance the energy flows. Such a plant acts as a thermal energy source. In networks where the sum of all prosumers results in a net annual cooling demand, a plant extracts thermal energy from the network in order to balance the energy flows. The plant in this case acts as a thermal energy sink. A typical example is a sewage plant. Large reservoirs, such as lakes, oceans or ambient air, are plants with an almost inexhaustible source or sink, respectively. Such plants thus supply or extract the thermal energy required by the prosumers at all times. If a large reservoir is present, usually no additional thermal storage is needed in the network.

Storage: A storage is an agent whose main task is to overcome the time shifts of heat supply to and heat extraction from the network. Integrated over one year, the net thermal energy transfer between network and storage is, ideally, zero (not taking into account storage heat losses). A storage thus only dampens the seasonal temperature fluctuations in the network, but does not contribute to its annual energy balance. Examples of storages are geothermal borehole fields, water tanks, aquifers, or phase change materials. The fluid and its related mass in the network piping[2] is also considered as a storage, even though their thermal storage capacity is typically much lower compared to other (seasonal type) storages.

[2] The non-insulated network piping in the ground also act as a geothermal heat exchanger. This storage effect was not taken into account in our simulations. In future research, this effect will be investigated and described in corresponding models.

4. Model of the network topologies

4.1. Network topology

In the base-case, which is a BN, the agents are connected in parallel between the two network pipes (Fig. 1a). The comparison considers a BN with three prosumers, one plant and one storage. Prosumers operating in heating mode draw water from the warm pipe and inject it into the cold pipe. Prosumers operating in cooling mode extract water from the cold pipe and inject it into the warm pipe. The direction of the mass flow through the prosumers thus switches depending on heating and cooling demand of the prosumers. The plant, in our case, supplies thermal energy into the network and thus always extracts water from the cold pipe and injects into the warm pipe. The residual mass flow is transported across the storage. The storage pump and control valves are operated to satisfy zero mass flow through the bypass (indicated by "m' = 0" in Fig. 1a). Recall that the mass flow in the bypass and the connection lines to the storage can be in both directions. Therefore, the storage contains switching valves that ensure that the borehole field has unidirectional mass flow.

The reservoir network (RN) is a thermal network with a one-pipe loop (Fig. 1b), the so-called reservoir loop. The agents take water from the reservoir loop to cover their heating or cooling demand and reinject the water back into the same reservoir loop. The extraction and reinjection points of the agents are next to each other along the same pipe, i.e. the reservoir loop. This concept ensures hydraulic decoupling of agent pumps and the reservoir pump. Because circulation pumps control the mass flow rates, no control valves and thus no hydraulic balancing is required. Whereas the flow in the cold and warm pipes of the BN can change direction, the flow direction in the reservoir loop remains constant and is defined by the flow direction of the reservoir pump. On the building level, the RN topology may be compared to one-pipe heating and cooling systems [30].

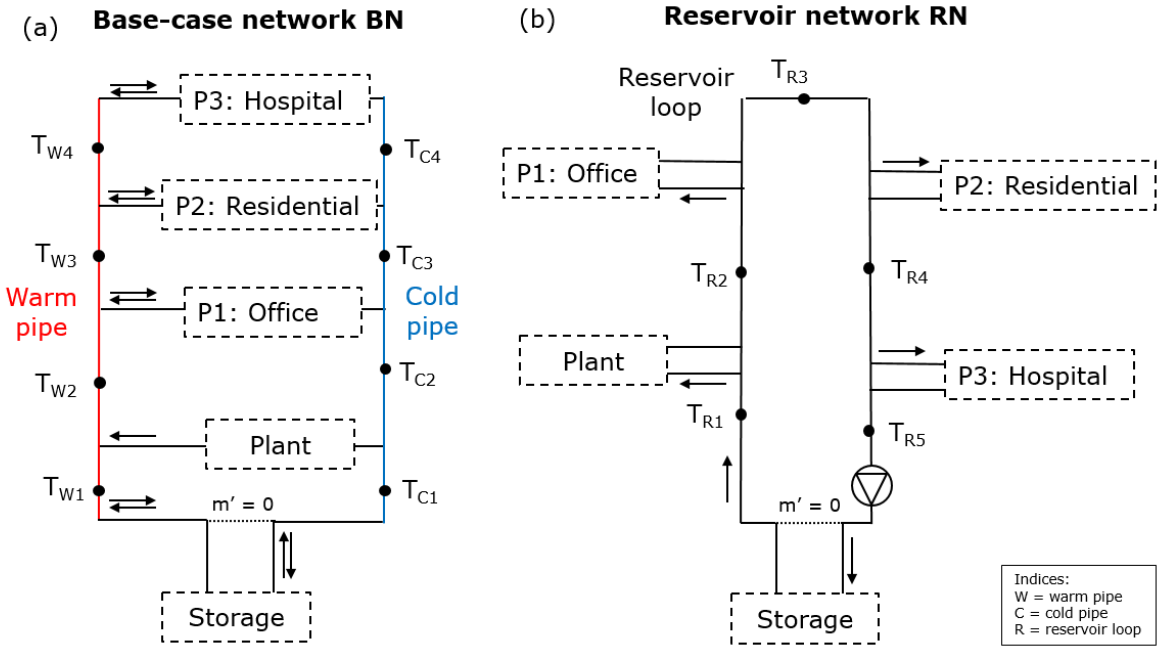

Fig. 1: Schematics of the bidirectional network (BN) and the reservoir network (RN). The arrows indicate the possible directions of mass flows through the agents and the network pipes. Temperatures are measured in the network pipes at the indicated points (e.g. T_{W1}).

4.2. Hydraulic integration of agents

For the prosumers, we use an office building, a residential building, and a hospital. The hydraulic schemes within the prosumers (Fig. 2a) are kept identical in the BN and the RN for comparison. During simultaneous heating and cooling within a prosumer, the prosumer internally recovers waste heat from cooling to be used for heating. Hence, only the residual heating or cooling demand (net heating demand) is exchanged with the network.

The network integration of the prosumers differs between the BN and the RN (Fig. 2b, c). In the BN, the temperature levels of the warm and the cold pipe must be kept separate. This requires a bidirectional mass flow through the prosumer depending on its heating or cooling demand (Fig. 2b). In the RN with unidirectional mass flow in the reservoir loop, the inflow water to the prosumer must always be taken upstream from and reinjected downstream into the reservoir loop. Otherwise, the mixing of outflow into inflow water reduces the efficiency of the RN prosumers. To ensure upstream extraction and downstream injection, various hydraulic schemes are possible. Fig. 2c shows one possible realization using two three-way valves.

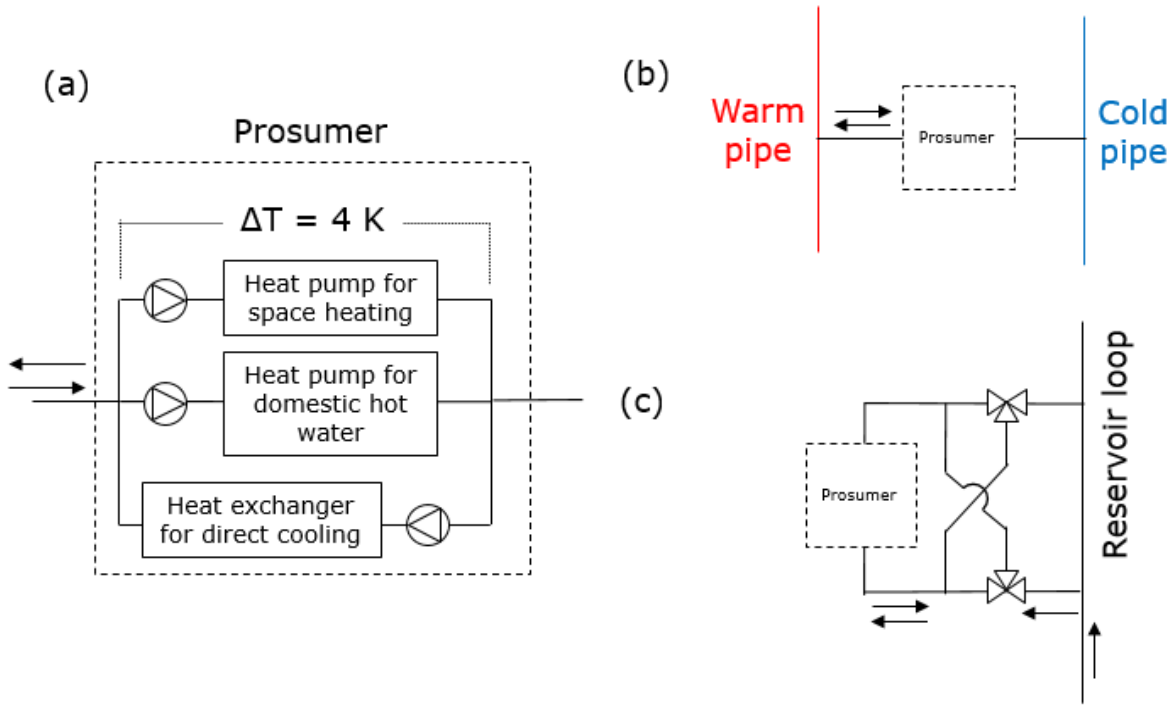

Fig. 2: Schematic of a prosumer and the prosumer connection to the network pipes. a, Schematic of a prosumer, valid for both the BN and the RN. The net mass flow rate depends on the heating and cooling demands of the prosumer and can change direction, indicated by the two arrows. **b,** Prosumer implementation in the BN. **c,** Prosumer implementation in the RN. The two three-way valves act as flow switches to ensure upstream extraction and downstream reinjection, at all times.

The plant is a sewage water heat exchanger (Fig. 3a). The network integration of this heat exchanger is parallel in the BN and serial in the RN. The plant only supplies heat into the network. Therefore, the heat exchanger's flow direction in both network topologies remains the same.

The storage is a borehole field with 350 probes connected in parallel (Fig. 3b). The network integration of the storage varies in the BN and the RN (Fig. 3c, d). In the BN, two three-way valves allow for unidirectional flow through the borehole field, despite the bidirectional flow in the warm and the cold pipe (Fig. 3c). In the RN, the three-way valves are not required as the mass flow in the reservoir loop is always unidirectional (Fig. 3d). In both integrations, the storage pump ensures zero mass flow through the storage bypass. In the BN, the storage bypass decreases the pressure difference between the warm pipe and the cold pipe and hence reduces pump-to-pump interactions between agents. In the RN, zero mass flow through the bypass ensures maximum thermal energy transfer between the storage and the network [31].

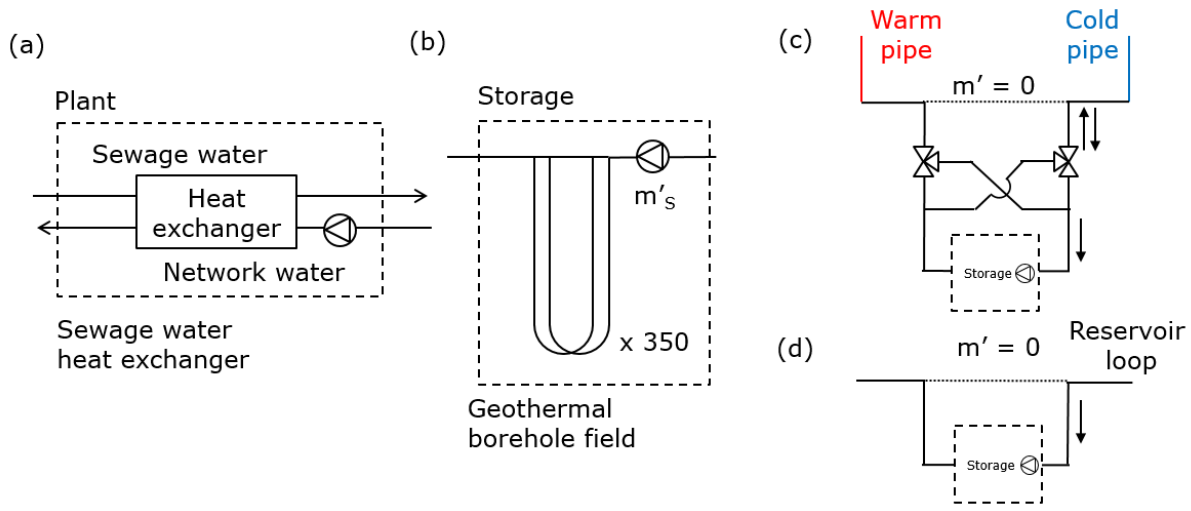

Fig. 3: Schematic of the plant, the storage and the storage connection to the network pipes. a, Schematic of the plant with a sewage water heat exchanger. **b**, Schematic of the storage with a borehole field. **c**, Storage implementation in the BN. The two three-way valves act as flow switches and enable a unidirectional mass flow through the storage, independent of the changing mass flow directions between the warm and the cold pipe. **d**, Storage implementation in the RN.

4.3. Sizing of network pipes and circulation pumps

Table 1 shows the main design parameters of the reservoir pumps and pipes. For the BN case, there is no main circulation pump and the mass flow rates through the warm and the cold pipes are a result of the mass flow rates through the prosumers and the plant and vary over time. The design mass flow rates for the pipe design are equal to the 95th percentile of the hourly mass flow rate distributions in the respective pipe sections. The pressure drop at design mass flow rate is 250 Pa m^{-1}. The resulting pipe diameters of the cold and warm pipes in the BN are 0.17 m, 0.18 m, 0.18 m and 0.11 m, according to the four pipe sections between the storage and prosumer P3 (Fig. 1a). The resulting average network pipe diameter in the BN is 0.17 m (Table 1).

For the RN1, RN2 and RN3 cases, we designed the mass flow rate in the reservoir loop to satisfy design conditions on temperatures, e.g. that the temperatures everywhere in the distribution loop must be between 6 °C and 17 °C, are violated during less than 0.1 % of all hours. Those design conditions can be fulfilled by different control strategies, assuming constant mass flow rates and also variable mass flow rate in the reservoir loop. The reservoir loop in scenario RN1 is operated with constant mass flow rate of 95 kg s^{-1} and assumes a pressure drop for 250 P m^{-1}. The resulting pipe diameter is 0.21 m. The scenario RN2 is operated also with a constant mass flow rate of 95 kg s^{-1} but considers a lower pressure drop of 125 Pa m^{-1} at design mass flow rate. This design adaption reduces circulation pump energy for the reservoir loop. The pipe diameter of RN2 is only slightly increased compared to RN1 to 0.23 m. In the third scenario RN3, the mass flow rate in the reservoir loop is controlled according to the network temperatures. The mass flow rate in the reservoir loop of RN3 is thus variable. As for the BN, the design mass flow rate for pipe design is defined by the 95^{th} percentile of the hourly mass flow rate distribution, here 69.5 kg s^{-1}. For a pressure drop of 250 Pa m^{-1} at design mass flow rate, the resulting pipe diameter of RN3 is 0.18 m. Circulation pump maximum design mass flow rates are equal to the maximum mass flow rates. Note that RN3 requires a slightly higher maximum circulation pump mass flow rate than RN1 and RN2. This is attributed to temperatures variations in the loop. The different network temperatures affect the COPs of the heat pumps in the prosumers and thus the mass flows through prosumers and in the reservoir loop.

Cases	Circulation pump design mass flow rate [kg s^{-1}]	Pipe design mass flow rate [kg s^{-1}]	Specific pressure drop R [Pa m^{-1}]	Resulting pipe diameter [m]
BN	n/a	n/a	250	average 0.17
RN1	95.0	95.0	250	0.21
RN2	95.0	95.0	125	0.23
RN3	97.3	69.5	250	0.18

Table 1: Design values for BN and RN. These values are used to parametrize the models for circulation pumps and pipes.

5. Models used for the analysis

Section 4 described the systems that were analysed. In this section, we explain the main physical assumptions and the main component models that have been used to conduct the analysis. All models are implemented using the equation-based, object-oriented Modelica language [32]. Component models from the Modelica Buildings Library version 6.0.0 [29] were used. Modelica has already been successfully used in the dynamic modelling of 4GDH [33,34] and 5GDHC networks [35,36] and was found to be better suited for these applications than alternatives like e.g. EnergyPlus because of its larger flexibility [37]. Each system model consists of about 7000 equations that form a differential algebraic system of equations. These equations were simulated using Dymola 2020 on Linux with the Radau solver and a tolerance of 1E-5. To control the accuracy of the simulation, this solver adapts the length of the time step, in our model typically between seconds and an hour. All simulations were done for a one year period.

5.1. Prosumers

Demand Profiles

The prosumers in both topologies, BN and RN, are a residential building, an office building, and a hospital, representing a typical mixed-use district. Each prosumer has predefined hourly demand profiles for space heating, domestic hot water and space cooling (Fig. 4). These demands are provided by the heat pumps and heat exchangers in the prosumers. All hourly profiles used in the simulation are based on Swiss archetypes [38–40] and scaled up to provide demand profiles for a typical Swiss district.

The heating demand (space heating plus domestic hot water) in the residential building is 2.40 GWh $year^{-1}$ (Fig. 4a). The average specific heating demand in new or retrofitted Swiss residential buildings is approximately 40 kWh m^{-2} $year^{-1}$ [41,42]. The specific floor area per person is, on average, 46 m^2 [43]. A heating demand of 2.40 GWh thus corresponds to a residential floor area of approximately 60'000 m^2 or 1'300 inhabitants.

The heating demand of the office building considered in this study is 0.19 GWh $year^{-1}$ or 8 % of the heating demand of the residential building (Fig. 4b). On average in Switzerland, the heating demand of office buildings is 4 % to 8 % of the heating demand of residential buildings. Hence, in our example, the ratio of the office to residential heating demand corresponds to a typical Swiss usage mix.

For the residential building and the office building, the ratio of annual heating to cooling demand is 7.8 and 2.1, respectively. The current ratio of heating to cooling demand in modern residential buildings is between 10 and 20 [3]. Considering future climate change, this ratio is expected to decrease to approximately 2 in 2060 [3]. The ratios of 7.8 and 2.1 thus represent an expected demand pattern on the pathway to 2060.

The hospital has a heating demand of 0.97 GWh $year^{-1}$ and a cooling demand of 0.23 GWh $year^{-1}$ (Fig. 4c). The ratio of heating to cooling demand is 4.3. In comparison to the residential or office demand profiles the main difference is the large share of domestic hot water.

In total for all prosumers, the heating demand is 3.55 GWh and the cooling demand is 0.62 GWh $year^{-1}$ (Fig. 4d). The overall ratio of heating to cooling demand for all prosumers is 5.7.

The model takes these demand profiles as a boundary condition and operates the energy transfer station in such a way that they are met.

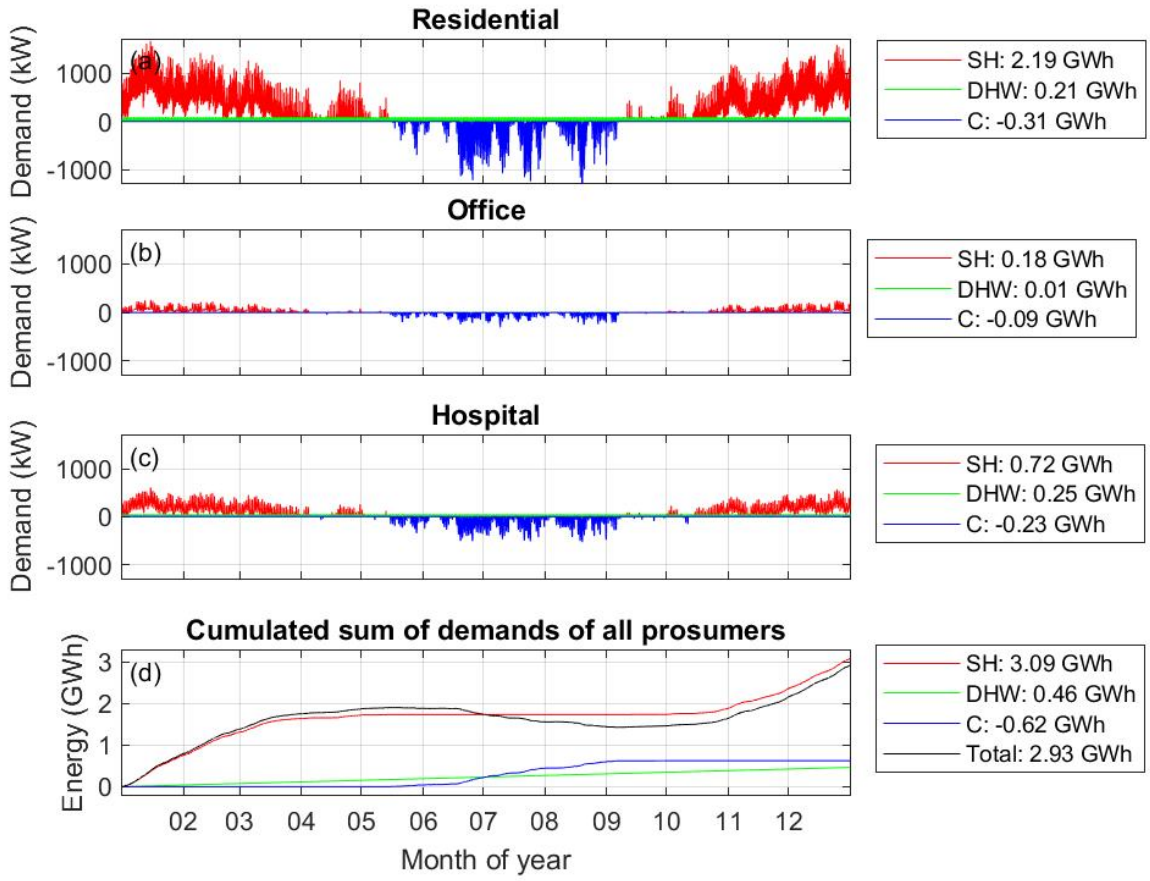

Fig. 4: Demand profiles for a Swiss residential building, an office building and a hospital. The legend indicates the annual space heating (SH), domestic hot water (DHW) and cooling demand (C), respectively. Panel (d) shows the total SH, DHW and C demands, represented by the cumulative sum. The net demand is a heating demand of 2.93 GWh.

Heat pumps and heat exchanger for cooling

Each prosumer uses a heat pump for space heating and a heat pump for domestic hot water. For space heating, we used a set point for the condenser outlet temperature of 38 °C at full demand, resetting this temperature to 28 °C at zero demand. For domestic hot water, the set point is 63 °C.

For the heat pumps, we used the model *Carnot_TCon*. This model has idealized internal control that causes the heat pump to track the set point of the water temperature leaving the condenser. It computes the heat pump COP as

$$COP = \eta_{carnot,0} \frac{T_{con}}{T_{con} - T_{eva}},$$

where $\eta_{Carnot,0}$ = 0.5 is the Carnot effectiveness, T_{con} is the condenser temperature and T_{eva} is the evaporator temperature. The model assumes the evaporator and condenser temperatures to be equal to the water outlet temperatures, with pinch temperatures of 2 K at design conditions. For off-design conditions, these pinch temperatures are scaled proportionally to the ratio of current heat flow rate at the evaporator (or condenser) divided by the design heat flow rate at the evaporator (or condenser).

Space cooling is provided as follows: As the prosumers receive, from the district loop, water at a temperature of at most 17 °C (see Section 5.2), we assume that heat exchangers provide direct cooling to meet the space cooling demand. Moreover, as the prosumers are obliged to ensure a 4 K maximal temperature shift of the network fluid (see also Section 5.2), we modelled direct cooling as a circulation pump and heat exchanger, whereas the circulation pump draws water in the amount of

$$\dot{m} = \frac{\dot{Q}}{c_p \, \Delta T},$$

from the cold side, where $\dot{Q}$ is the space cooling demand, c_p is the specific heat capacity of water and $\Delta T = 4$ K is the temperature difference. The heat exchanger then extracts $\dot{Q}$ from this water flow rate and the water is fed to the warm side. Because we did not model the building-side of the heat exchanger, this approach suffices to model the physical behaviour that affects the thermal network.

Mass flow rates and flow friction

The mass flow rates on the network side of the heat pumps and heat exchangers are designed and controlled to satisfy a temperature difference between inflow and outflow of the heat pumps and the heat exchangers of $\Delta T = 4$ K.

The hydraulic resistances in the prosumers and the plant in both networks BN and RN are designed assuming a pressure drop of 50 kPa at design mass flow rate. The pressure drop due to the connection lines between the prosumer and the network are included in the 50 kPa pressure drop of the prosumer.

For off-design conditions, mass flow rate $\dot{m}$ and pressure drop Δp are related as

$$\dot{\mathrm{m}} = \mathrm{sign}(\Delta \mathrm{p}) \, \mathrm{k} \sqrt{|\Delta \mathrm{p}|},$$

where k is a fixed coefficient computed based on the design mass flow rate and pressure drop. For low flow rates, the model transitions toward laminar flow.

5.2. Plant and Storage

In both BN and RN topologies, the plant and the storage must fulfil two design conditions:

(i) Energy: The annual energy balance of the storage is zero. Thus, on a yearly basis, the plant covers the heating and cooling demands that all prosumers impose on the network pipes (minus the circulation pump energy).

(ii) Capacity: The prosumers must be supplied with temperatures between 6 °C and 17 °C. The upper limit of 17 °C enables direct-cooling. The lower limit of 6 °C ensures that the water is still above freezing temperature, assuming a temperature decrease of 4 K by the heat pumps.

Various design options for the plant and storage are possible to fulfil boundary conditions (i) and (ii). Because the focus of this work is a comparison between topologies and not the cost optimized design of plant and storage, we have chosen a simple but realistic set-up to fulfil the boundary conditions:

The plant is a sewage water heat exchanger. The sewage water has a constant inflow temperature of 17 °C and a constant mass flow rate of 11.45 kg s^{-1}. The mass flow rate on the network side of the sewage water heat exchanger is also 11.45 kg s^{-1} to make optimal use of the heat exchanger. The heat exchanger effectiveness ε is a measure for the heat exchanger size, which is a design parameter to fulfil design condition (i) and hence differs between the BN and the RN. The hydraulic resistance in the plant in all networks is 50 kPa at design mass flow rate.

For the sewage water heat exchanger, we used the model *ConstantEffectiveness*. This model transfers heat according to

$$Q = Q_{max}\,\varepsilon,$$

where ε is a constant effectiveness and Q_{max} is the maximum heat that can be transferred, computed as

$$Q_{max} = C_{min}\,|T_{in1}-T_{in2}|,$$

where C_{min} is the lower of the capacity flow rates of the two fluid streams and $|T_{in1}-T_{in2}|$ is the difference in inlet temperatures.

The storage is a borehole field with 350 double U-tube probes of 250 m depth. The ground temperature is 9.4 °C in the top 10 m. From 10 m to 250 m depth, the ground temperature increases by 0.02 °C m^{-1} from 9.4 °C to 14.2 °C. The borehole field has a pressure drop of 35 kPa at a design mass flow rate of 105 kg s^{-1}, i.e. 0.3 kg s^{-1} in each probe.

For the borehole field, we used the model *TwoUTubes*. This model is based on the following key assumptions: the thermal properties of the soil (conductivity and diffusivity) are constant, homogenous and isotropic. The conductivity, capacitance and density of the ground and pipe material are constant, homogenous and isotropic. There is no heat extraction or injection prior to the start of the simulation. All boreholes in the borehole field have uniform dimensions (including pipe dimensions). Inside the boreholes, the non-advective heat transfer is in the radial direction only.

The borehole field models are constructed in two main parts: the boreholes, and the ground heat transfer. The boreholes are modelled as a vertical discretization of borehole segments, all of them sharing a common uniform borehole wall temperature. The thermal effects of the circulating fluid (including the convective resistance), pipes and filling material are all taken into consideration, which allows the modelling of short-term thermal effects in the borehole. The borehole segments do not take into account axial effects, thus only radial (horizontal) effects are considered. The thermal behaviour between the pipes and borehole wall are modelled using a resistor-capacitor network. The second main part of the borehole field model is the ground heat transfer, which shares a thermal boundary condition at the uniform borehole wall with all of the borehole segments. The heat transfer in the ground is modelled analytically as a convolution integral between the heat flux at the borehole wall and the borehole field thermal response factor.

5.1. Network pipes

To model the network pipework, we used the *PressureDrop* model. This model computes the flow resistance using a fixed flow coefficient k which is computed based on a user-specified pressure drop at a user-specified design flow rate. If there is a circulation pump in the flow leg, then the mass flow

rate is forced by the circulation pump, otherwise it is computed as $\dot{m} = sign(\Delta p)\ k\sqrt{|\Delta p|}$, with regularization for small flow rates, where Δp is the pressure drop across the flow leg.

5.2. Circulation pumps

The circulation pumps provide the necessary mass flow rates at all times by overcoming the corresponding pressure loss. The electric power required is determined by the resulting hydraulic power, taking into account both the circulation pump and the motor efficiency.

For the circulation pumps, we used the model *FlowControlled_m_flow*. We assumed a constant motor efficiency and constant hydraulic efficiency of $\eta_h = \eta_m = 0.7$. Hence, the electric power of the circulation pump is computed as

$$P = \dot{V}\ \Delta p/\eta_h/\eta_m,$$

where $\dot{V}$ is the volume flow rate and Δp is the differential pressure created by the circulation pump. Both, $\dot{V}$ and Δp are computed using a full flow versus pressure drop calculation in the whole flow network that is solved at each simulation time step.

5.3. Circulation pump control in the RN3 network

For the control of the main circulation pump in the RN3 network, we developed a controller that adjusts the pump speed. The controller reduces the pump speed unless the water temperature at the mixing points after the agents in the district is too high or too low, in which case the pump speed is increased to keep the loop temperature between a lower and upper bound. The control is as follows: Let T_{MixMin} and T_{MixMax} be the minimum and maximum measured mixing temperatures and let T_l and T_u be the lower and upper bounds for the mixing temperatures. If $T_{MixMin} - T_l > 2K$ or $T_u - T_{MixMax} > 2\ K$ then the pump speed is set to the minimum speed y_{PumMin}. Otherwise it is linearly increased to the full speed until $T_l = T_{MixMin}$.or $T_u = T_{MixMax}$. This calculation is done for the lower and upper bound, and the actual pump speed is the larger of the two pump signals. This reset of the mass flow rate reduces circulation pump energy while meeting design condition (ii) above.

6. Comparison

To compare the performance, we conducted annual simulations with hourly time resolution. Beside the BN simulation, three scenarios are simulated and evaluated in order to show the performance drivers in the RN. RN1 considers the same pipe dimensioning as in the BN, but operates with a constant mass flow rate for the reservoir loop. RN2 is equal to RN1, but considers a lower pressure drop than RN1, resulting in a larger pipe diameter. RN3 takes into account a mass flow rate control for the reservoir loop, with the same pipe dimensioning as in the BN or RN1, respectively.

The externally supplied energy in both cases is electric energy from the public grid. Using the CO_2 associated with one kWh of site electric energy, the CO_2 impact could be estimated. The study does not undertake any calculations in this respect, because the seasonal patterns of electric energy consumption do not vary significantly among the cases under consideration. For this reason, the difference in electric energy demand is representative of the difference in CO_2 impact. In contrast, the flexibility of the electric energy demand in the daily demand profile offers potential in all cases for CO_2 reduction. Such evaluations would have to be investigated by further studies.

The economic performance is assessed on the basis of investment costs (CAPEX). Because the same depreciation period of the components in the BN and RN is assumed, only investments can be compared. Operating costs (OPEX) are considered only by assessing electric energy demand. This is appropriate because maintenance costs for both network topologies BN and RN are judged to be similar.

7. Results

7.1. Compliance with design conditions

The prosumers have a net annual heating demand of 2.93 GWh (Fig. 5a). This demand is covered partially by thermal energy transferred by the plant into the network pipes and partially by the electric energy of the heat pumps. In the BN, the plant supplies 2.214 GWh $year^{-1}$. In the RN3[3], the plant supplies 2.210 GWh $year^{-1}$ (Fig. 5b, red lines). The small difference of the plant's energy supply between the BN and the RN3 already indicates that the heat pumps on average across all buildings are operating at similar efficiencies in both topologies. The annually supplied thermal energy from the plant to the network is equal to annually extracted thermal energy from the network by the prosumers (Fig. 5b, solid black lines). Consequently, the annual energy supply by the storage is zero and design condition (i) is fulfilled for both topologies (Fig. 5b, dotted black lines).

The network temperatures and hence the coefficients of performance (COPs) of each prosumer are different in the BN and the RN. The plant heat exchanger effectiveness (related to the size of the heat exchanger) was therefore adapted to meet design condition (i). The resulting heat exchanger effectiveness is 0.70 in the BN and 0.94 in the RN1 and RN2. In the RN3, the heat exchanger effectiveness is 0.91.

Figure 5b also provides an understanding of the energy balance throughout the year. The plant continuously transfers heat into the network (positive slope of the red line in Fig. 5b) and acts as a source. The storage supplies thermal energy to the network in the beginning of the year (positive slope of the black solid line in Fig. 5b). During spring and autumn, the energy transfer is close to zero. During summer, the storage extracts thermal energy from the network (negative slope of the black dashed line in Fig. 5b).

The prosumers extract thermal energy from the network in the heating period (negative slope of the black solid line). In summer, during the cooling period, the prosumers supply waste heat from cooling (positive slope) to the network. This waste heat is stored in the borehole field (negative slope of the black dashed solid line Fig. 5b). In autumn, the heating period with heat extraction by the prosumers starts again. Over one year the prosumers extract more thermal energy from the network than they supply. The plant covers the heat deficit, as mentioned above.

[3] Only the results of RN3 are shown in the graphical evaluation. For RN1 and RN2, the findings can be applied similarly.

During the entire year, the network temperatures range between 6 °C and 17 °C in both the BN and the RN3. Design condition (ii) is thus also fulfilled (Fig. 5c, d). RN2 and RN3 also fulfil the design conditions (ii), but are not shown in Fig. 5.

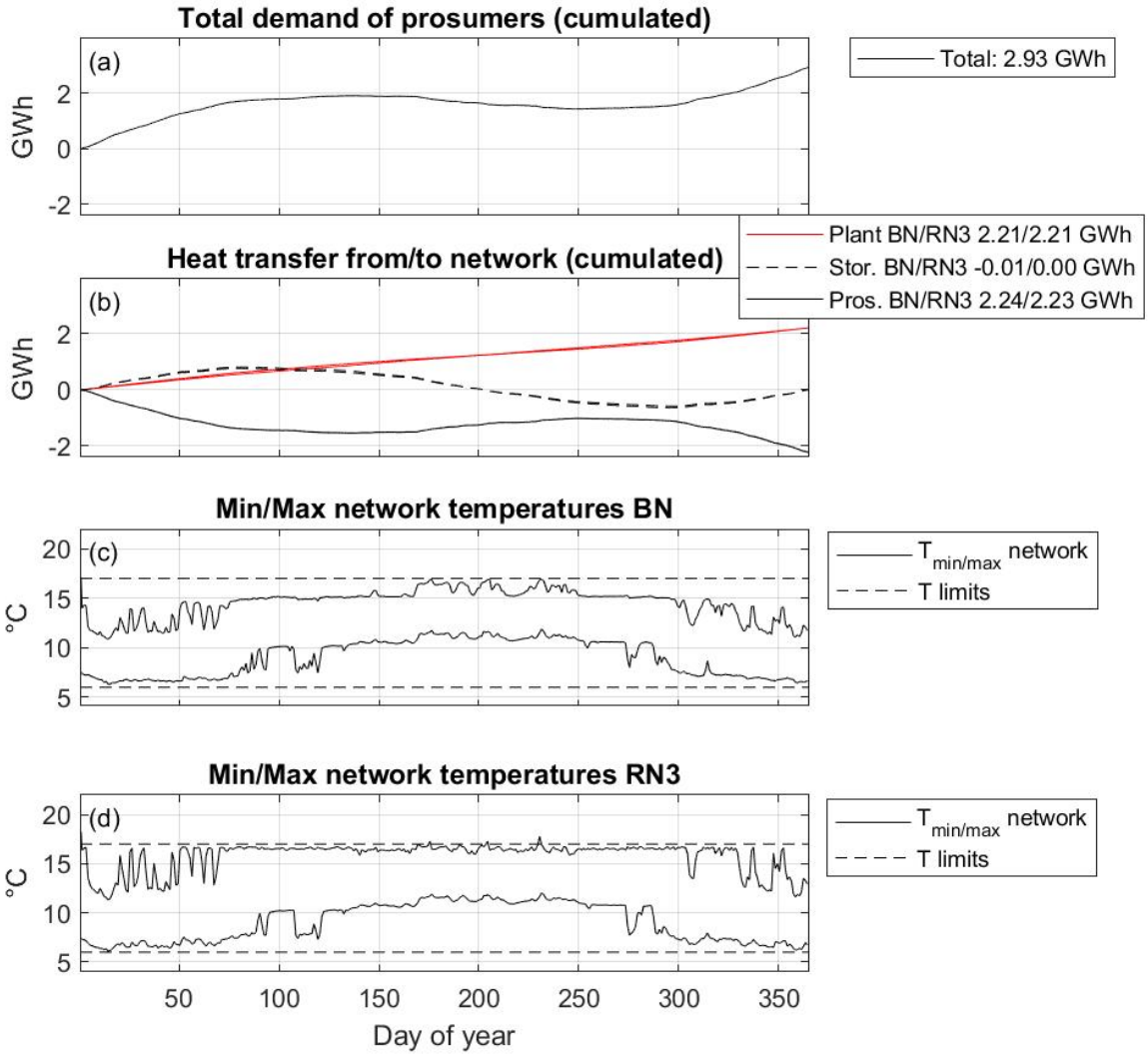

Fig. 5: Visualization of the design conditions for the plant and the storage. a, Net demand of prosumers, shown as cumulative sum for reference (identical to black line in Fig. 4d). **b,** Heat supply to network, shown as cumulative sum for the plant, storage and all prosumers. The curves of the BN and the RN3 lie on top of each other and can hardly be distinguished. **c,d** Daily minimum and maximum temperatures in the network pipes of the BN (c) and the RN3 (d). The dashed horizontal lines indicate the temperature limits of design condition (ii).

7.2. Mass flow rates and heat pump performance

The mass flow rates through the prosumers in the BN and the RN3 vary according to the COPs of the heat pumps (Fig. 6a). The different COPs in the BN and RN3 result from different supply temperatures. The mass flow rate through the plant is identical in the BN, RN1, RN2 and RN3. In the

BN, the mass flow rates through the network pipes and the storage are determined by the net mass flow rates through the prosumers and thus vary depending on demand (Fig. 6a). In the RN1 and RN2, the mass flow rate through the reservoir loop is constant at 95 kg s^{-1} (not shown in Fig. 6). In the RN3 scenario (Fig. 6a), the mass flow rate in the reservoir loop is defined by the circulation pump control and varies in order to minimize the mass flow rate and still meet design condition (ii).

The hourly COPs of the heat pumps for space heating vary between 4.1 and 12.3. The hourly COPs of the heat pumps for domestic hot water are between 2.7 and 3.4. The COPs in the RN3 differ only slightly to the COPs in the BN (black and green boxes in Fig. 6b). The COP differences occur because of different supply temperature to the heat pumps from the BN or RN, respectively (Fig. 5c,d).

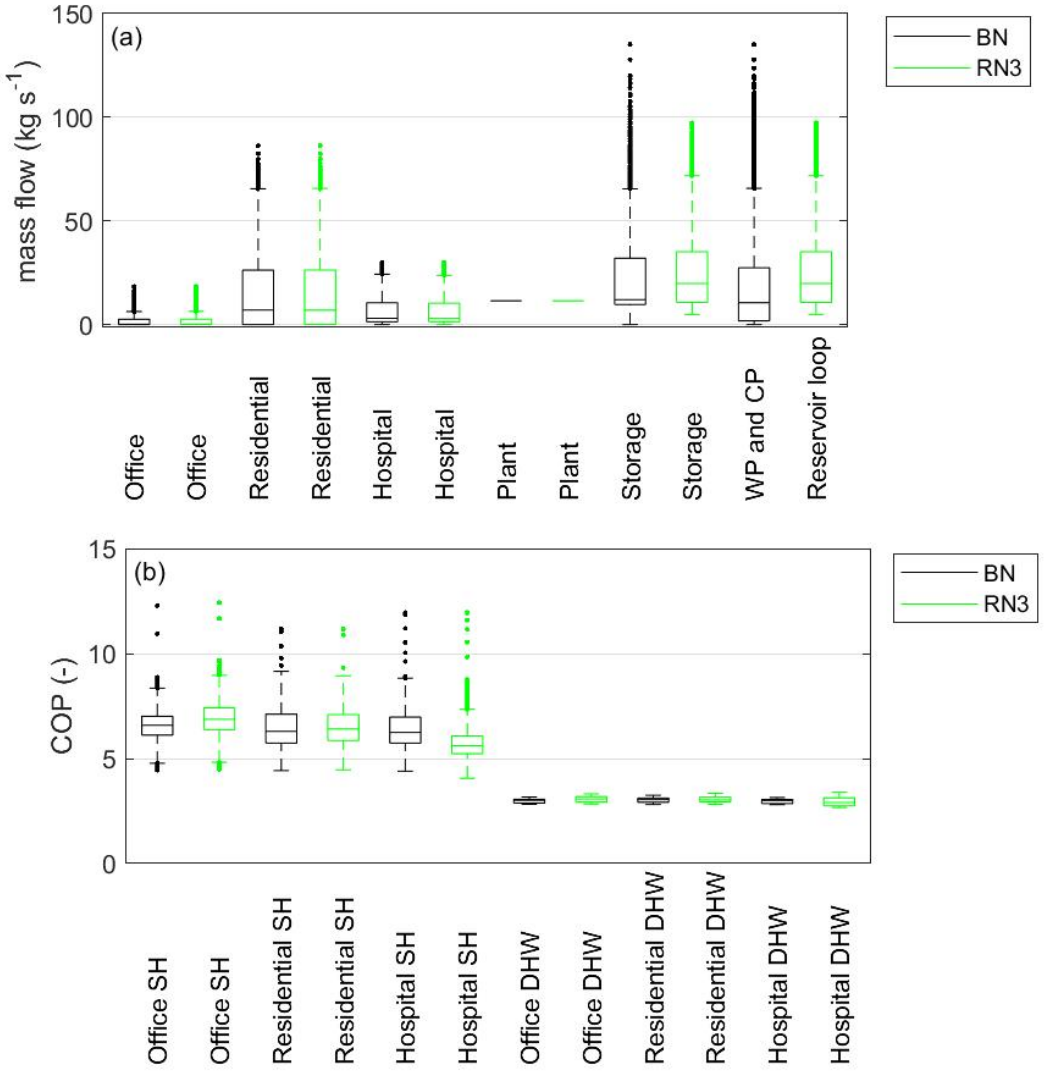

Fig. 6: Mass flow rates and COPs in the BN and the RN topology. a, Mass flow rates through the network and agents in the BN (black) and the RN3 (green), represented by box plots. The limits of a box define the 25 and 75 percentiles of the distribution. 50 % of the data is therefore represented within a box. The horizontal line in a box represents the median of the distribution. The whiskers contain 99.3 % of the data (for normally distributed data) and the dots are the outliers. **b,** Box plots of the COPs of the prosumer's heat pumps. Only COPs with mass flows larger than 0.1 kg s^{-1} on the evaporator side of the heat pump are evaluated.

7.3. Electric energy consumption

The main evaluation criterion for the comparison is the electric energy consumption of the heat pumps and the circulation pumps. The annual electric energy E consumed by the heat pumps is 0.69 GWh in the BN, 0.70 GWh in the RN1 and RN2 scenarios and 0.69 GWh in the RN3 scenario (Fig. 7a). The annual electric energy consumed by the circulation pumps is 0.07 GWh in the BN, 0.42 GWh in the RN1, 0.25 GWh in the RN2 and 0.06 GWh in the RN3. RN1 and RN3 have the same specific pressure drop of 250 Pa m^{-1}. The large circulation pump energy in the RN1 is thus caused by the large, constant mass flow rate in the reservoir loop and the storage. Decreasing the specific pressure drop to 150 Pa m^{-1} by increasing the pipe diameter in the RN2 reduces the circulation pump energy compared to RN1, but still results in a larger circulation pump energy compared to the RN3. In the RN3, with temperature-dependent mass flow rate control, the circulation pump energy is similar to the BN.

The seasonal dynamics of the electric energies for heat pumps show the expected pattern with large electric energy consumption in winter for space heating and domestic hot water and small electric energy consumption in summer for domestic hot water only (Fig. 7b, c, d, e). The circulation pump energy is approximately constant in RN1 and RN2 throughout the year, because the control of the mass flow rates in the reservoir loop are equal and constant in both scenarios. In the BN and the RN3, mass flow rates (and thus circulation pump energies) are largest in winter (for heating) and in summer (for cooling) and smallest in the intermediate seasons. However, in BN and RN3, the circulation pump energy is still small compared to the heat pump energy and thus only marginally influence the seasonal pattern of total energy consumption.

Circulation pump energy is extremely sensitive to the design diameter of the piping system, i.e. being proportional to the inverse of the pipe diameter to the 5^{th} power. By using larger pipe diameters than the design values, the circulation pump energy can be reduced significantly. Calculations for scenario RN2 show that by increasing the pipe diameter of the reservoir loop by 14 %, from 0.21 m (corresponding to 250 Pa m^{-1} specific pressure drop) to 0.23 m (125 Pa m^{-1}), the annual circulation pump energy is reduced by 40 %, from 0.42 GWh to 0.25 GWh (Fig. 7, second and third bar).

In summary, the annual energy consumption by heat pumps and circulation pumps is 0.76 GWh in both the BN and in the RN3. However, pipe diameters are 0.17 m and 0.18 m in BN and RN3 respectively. The RN, if operated at controlled mass flow rates depending on the network temperatures, is thus comparable to the BN in terms of energy efficiency. When the RN is operated at a constant mass flow rate, the circulation pump energy and the overall electric energy consumption will increase dramatically. The RN should therefore always be operated at variable mass flow rates (dependent on network temperatures) to fulfil design condition (ii). Consequently, both network topologies can be operated with similar electric efficiency and thus CO_2 impact. The operational costs (OPEX) are also expected to be approximately the same because of similar maintenance and energy costs.

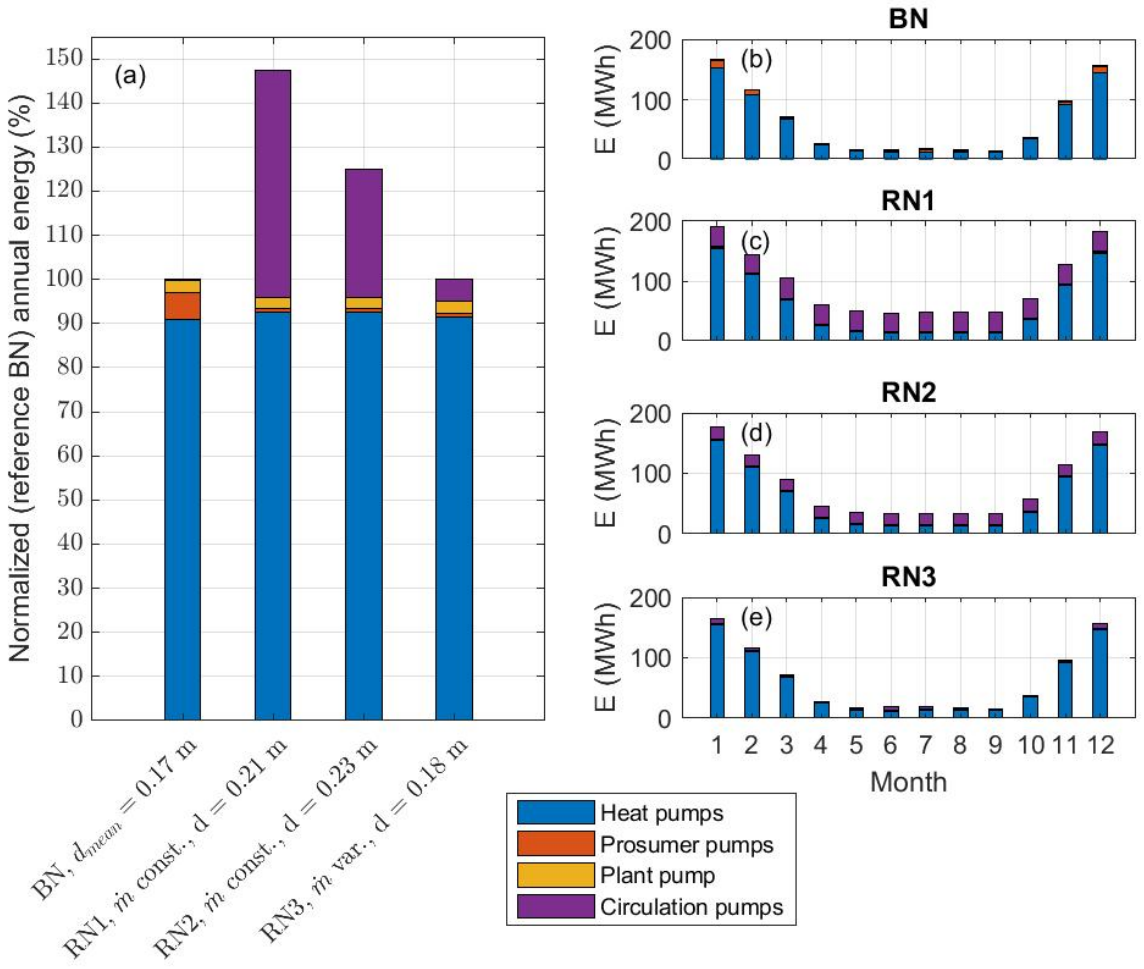

Fig. 7: Electric energy consumption of the heat pumps and the circulation pumps for the different scenarios. a, Annual electric energy for heat pumps and circulation pumps. Note that on the left axis, the annual electric energy consumption of the BN is normalized to 100 %, equalling 0.76 GWh year^{-1}. In the BN, "Circulation pumps" in the legend (violet) refers only to the storage pump. In the RN, "Circulation pumps" refers to both storage and reservoir pumps. The labels of the x-axis indicate the main characteristics of the different scenarios (mass flow rate in the reservoir loop and pipe diameters of the network pipes). **b to d**, Seasonal variability of the electric energy consumption for the four studied scenarios. Each bar corresponds to electric energy integrated over one month.

7.4. Installation costs

The results show that the electric energy consumption of the heat pumps in the BN and the RN is almost identical. The main difference in total electric energy consumption in the different scenarios of the RN is caused by the electric energy consumption of the circulation pumps. The electric energy consumption of the circulation pumps depends on the pipe diameters and the mass flow rates (see 7.3). For example, increasing the pipe diameter by a factor of 2 reduces circulation pump energy by approximately a factor of 2^5 = 32. Increasing the pipe diameter is thus an efficient measure to

decrease circulation pump energy or a measure for allowing larger mass flows at the same circulation pump energy.

However, increasing the diameter also increases the outlay costs, consisting of piping, trenching and installation. Trenching costs are assumed to be 800 EUR m^{-1} for a double pipe with diameters smaller than 0.4 m and 1000 EUR m^{-1} for pipe diameters between 0.4 and 0.8 m. For a single-pipe, trenching costs are 150 EUR m^{-1} less than for the double-pipe installation. Piping costs (including installation) vary, according to pipe diameter, between 70 and 400 EUR m^{-1} for a single pipe with (inner) pipe diameters between 220 mm and 500 mm. These cost estimates are based on market prices (personal communication with Lauber-Iwisa, Naters, Switzerland).

Figure 9 shows the outlay costs (trenching, installation and piping) in dependence of pipe diameter for a single-pipe and a double-pipe installation. The single-pipe configuration is less expensive than the double-pipe layout, even when the diameter of the single pipe is increased. For example, outlay costs for a double-pipe installation with diameter 200 mm are equal to a single-pipe installation of diameter 390 mm, both costing 900 EUR m^{-1}. In this case, the single-pipe network can afford to have a 95 % larger pipe diameter than a double-pipe system.

In the BN, the average diameter of the warm and the cold pipe sections is 0.17 m. In the RN cases, the pipe diameters of the reservoir loop vary between 0.18 and 0.23 m. The pipe diameters of the RN are 6 % to 35 % larger than those of the BN. The RN in single-pipe configuration can therefore be installed more cost-effectively than a BN with double-pipe configuration.

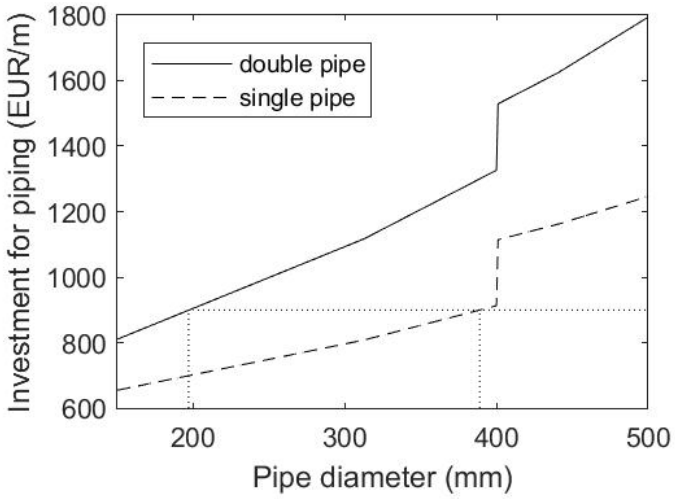

Fig. 8: Investment costs for piping as a function of pipe diameter for a PE100 pipe of pressure rating PN10. (Data: personal communication Lauber-Iwisa, Naters, Switzerland, conversion rate: 1 EUR = 1.1 CHF). The line for a double-pipe network was obtained by multiplying the cost for one pipe by a factor of two plus trenching costs. The horizontal dotted line indicates a price of 900 EUR/m. The vertical dotted lines indicate the diameters of the double-pipe (left) and the single-pipe (right) network for equal costs. The abrupt increase in investment costs at diameter 0.4 m is caused by the fixed increase in trenching costs.

In a circular district layout, the network pipes form a ring (Fig. 9 a,b). While the BN requires a double ring consisting of both a warm and a cold pipe, the reservoir loop requires only a single ring. We expect that a single-pipe system with up to 95 % larger diameters will be cheaper than a double-pipe system. However, in a linear district layout (Fig. 9 c,d), the pipe lengths of the BN and RN topologies are approximately equal and both can be considered to be a double-pipe system. In this case, the RN topology with its larger diameters will be more expensive. In conclusion, the economic advantage (CAPEX) of an RN over a BN configuration depends on the spatial layout of the network in the district.

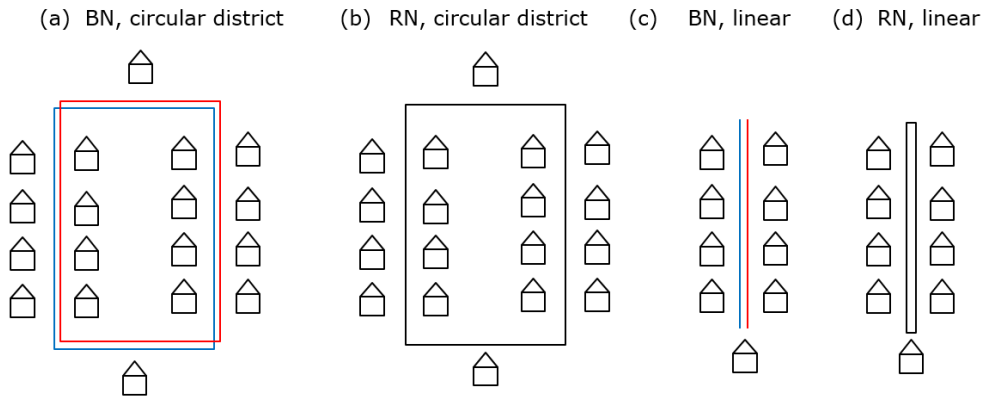

Fig. 9: Pipe length in the BN and the RN in dependence of the district structure. **a,b,** In a circular arrangement, the RN is a single-pipe system and the BN is a double-pipe system. **c,d,** In a linear arrangement, the pipe lengths of the RN and the BN are approximately equal and both systems are considered double-pipe systems.

8. Conclusion and Outlook

In this work, we compared two 5th Generation of District Heating and Cooling (5GDHC) systems involving five agents. In the base-case, which is a double-pipe, bidirectional network (BN), the agents are connected in parallel between a warm and a cold pipe. In the new reservoir network (RN), the agents are connected in series to a single-pipe reservoir loop.

We showed that the heat pumps in the RN have a slightly higher electric energy consumption due to lower network temperatures but the difference is less than 2 % for all three RN scenarios studied. The electric energy demand of the circulation pumps strongly depends on the pipe diameter and the mass flow rates. By using a variable mass flow rate controller for the reservoir loop circulation pump, the annual difference in electric energy consumption for heat pumps and circulation pumps between BN and RN is less than 1 %. However, we have also shown that an RN with constant mass flow rate requires massively more circulation pumping energy, causing the total electric energy consumption to increase by 48 % compared to the BN.

Districts with a circular network layout and a single-pipe RN require only half the pipe length than a double-pipe BN. An increase in diameter of up to 95 % of the RN compared to the BN can be accepted while still maintaining an economic advantage. For the RN with variable reservoir mass flow

rate, a slight increase in pipe diameter by 6 % over the BN average diameter leads to the most economical solution. In districts with a linear network layout, i.e. same pipe lengths for BN and RN, the economic difference is negligibly small.

In summary: An RN with variable mass flow achieves a comparable energy efficiency as a BN. In a distribution area with circular arrangement of the supply lines, there are economic advantages for the RN. With a linear arrangement of the supply lines, both topologies are similarly expensive to install and operate.

Additional advantages of the RN topology over conventional networks are its greater freedom in planning, its simplicity regarding further spatial extension of the network, and its robust operation. Performance adjustments in a prosumer, for example, can be achieved without adjusting hydraulic balancing valves in the network. Prosumers, plant and reservoir loop can adjust their mass flow rates without affecting the hydraulics of other prosumers. Further, various reservoir loops, even at different temperatures, may be connected in order to transport thermal energy across districts. The coupling can either be direct (red and yellow loop in Fig. 10) or indirect using a connection loop (dashed loop between the blue and the red loop in Fig. 10). The modular structure with interconnected loops allows simple network adaption and expansion [23].

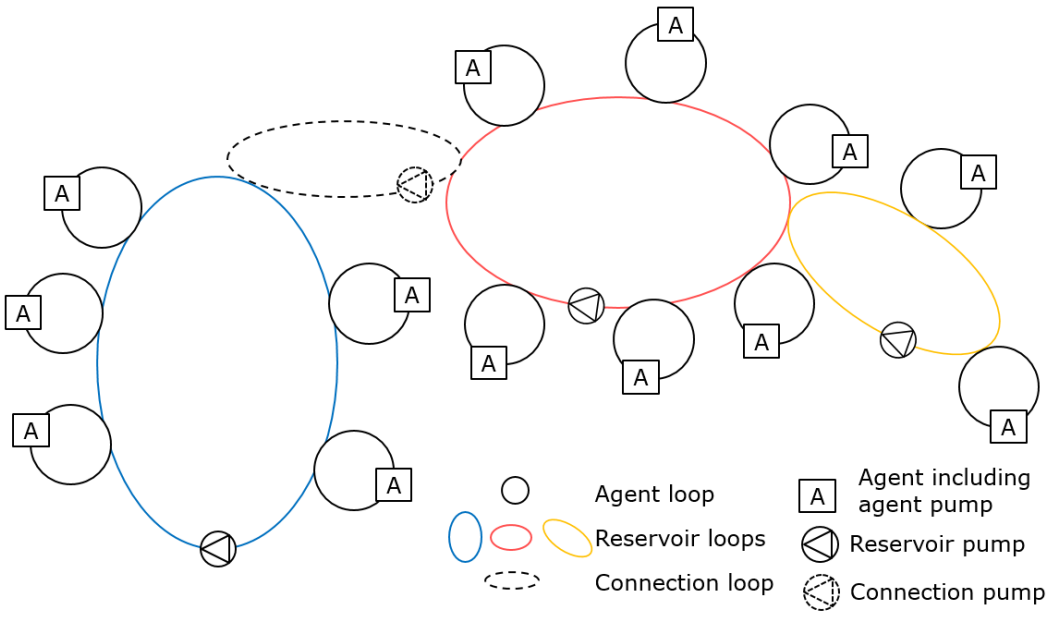

Fig. 10: Schematic of the reservoir network. The agents (black, connected to agent loops) exchange thermal energy with the reservoir loop (blue, red, and yellow colours indicate reservoir loops with different temperatures). The blue and red reservoir loops are connected indirectly with a connection loop (black dashed). The red and yellow reservoir loops are connected directly. Each loop has its own circulation pump. The circulation pumps in the agent loops are included in the agents (A). In this work, only one reservoir loop with five agents is studied, corresponding, for example, to the blue loop and the five connected agents.

This new RN topology will require more research to investigate broad application in different climate zones, urban morphologies and demand profiles. The geothermal potential on the uninsulated pipes must also be studied in detail in order to assess the storage capacity of the network as a whole. In addition, tools must be developed in order to plan, design and operate district heating and cooling concepts quickly, economically and with high reliability.

9. Author contributions

Tobias Sommer: Conceptualization, Data curation, Investigation, Formal analysis, Methodology, Supervision, Visualization, Roles/Writing - original draft, Writing - review & editing. **Matthias Sulzer:** Conceptualization, Formal analysis, Investigation, Methodology, Supervision Roles/Writing - original draft, Writing - review & editing. **Michael Wetter:** Conceptualization, Formal analysis, Methodology, Supervision, Software, Validation, Roles/Writing - original draft, Writing - review & editing. **Artem Sotnikov:** Formal analysis, Methodology, Software. **Stefan Mennel:** Project administration, Writing - review & editing. **Christoph Stettler:** Methodology, Investigation

10. Acknowledgements

The authors thank Kristina Orehounig and Portia Murray for providing demand profiles from the EnTeR Project [23].

This research project is financially supported by the Swiss Innovation Agency Innosuisse and is part of the Swiss Competence Center for Energy Research SCCER FEEB&D.

This research was supported by the Assistant Secretary for Energy Efficiency and Renewable Energy, Office of Building Technologies of the U.S. Department of Energy, under Contract No. DE-AC02-05CH11231.

This work emerged from the IBPSA Project 1, an international project conducted under the umbrella of the International Building Performance Simulation Association (IBPSA). Project 1 will develop and demonstrate a BIM/GIS and Modelica Framework for building and community energy system design and operation.

11. Data availability

All models are available in the package Buildings.Examples.DistrictReservoirNetworks of the Modelica Buildings library at https://github.com/lbl-srg/modelica-buildings, commit cf8fa64ac2ce792b7b81fa0064def2fb531e7833.

12. References

[1] Connolly D, Lund H, Mathiesen B V., Werner S, Möller B, Persson U, et al. Heat roadmap Europe: Combining district heating with heat savings to decarbonise the EU energy system. Energy Policy 2014;65:475–89. doi:10.1016/j.enpol.2013.10.035.

[2] Hansen K, Connolly D, Lund H, Drysdale D, Thellufsen JZ. Heat Roadmap Europe: Identifying the balance between saving heat and supplying heat. Energy 2016;115:1663–71. doi:10.1016/j.energy.2016.06.033.

[3] Settembrini G, Domingo S, Heim T, Jurt D, Zakovorotnyi A, Seerig A, et al. ClimaBau – Planen angesichts des Klimawandels. Bern: Bundesamt für Energie; 2017.

[4] Werner S. European space cooling demands. Energy 2016;110:148–56. doi:10.1016/j.energy.2015.11.028.

[5] Werner S. International review of district heating and cooling. Energy 2017;137:617–31. doi:10.1016/j.energy.2017.04.045.

[6] Rezaie B, Rosen MA. District heating and cooling: Review of technology and potential enhancements. Appl Energy 2012;93:2–10. doi:10.1016/j.apenergy.2011.04.020.

[7] Frederikson S, Werner S. District Heating and Cooling. Lund: Studentlitteratur AB; 2014.

[8] Lund H, Werner S, Wiltshire R, Svendsen S, Thorsen JE, Hvelplund F, et al. 4th Generation District Heating (4GDH). Integrating smart thermal grids into future sustainable energy systems. Energy 2014;68:1–11. doi:10.1016/j.energy.2014.02.089.

[9] Lund H, Østergaard PA, Chang M, Werner S, Svendsen S, Sorknæs P, et al. The status of 4th generation district heating: Research and results. Energy 2018;164:147–59. doi:10.1016/j.energy.2018.08.206.

[10] Buffa S, Cozzini M, D'Antoni M, Baratieri M, Fedrizzi R. 5th generation district heating and cooling systems: A review of existing cases in Europe. Renew Sustain Energy Rev 2019;104:504–22. doi:10.1016/j.rser.2018.12.059.

[11] Cozzini M, Trier D, Bava F, Fedrizzi R, Buffa S, Jensen LL, et al. FLEXYNETS Guide Book. Hochschule für Technik Stuttgart; 2018.

[12] Gemperle S, Trecco S. «Thermische Netze» – Entscheidungskriterien für die Systemwahl. EnergieSchweiz; 2018.

[13] Ködel J, Hangartner D. Fallbeispiele "Thermische Netze" 2018. https://www.energieschweiz.ch/home.aspx?p=22949,22963,22985.

[14] Gaudard A, Schmid M, Wüest A. Thermische Nutzung von Oberflächengewässern. Aqua Gas 2017;5:40–5.

[15] Gaudard A. Thermische Nutzung von Seen und Flüssen 2018. https://thermdis.eawag.ch/de/map-installations.

[16] Stettler C, Schluck T, Sulzer M, Sommer T. Electricity Consumption of Heat Pumps in Thermal Networks depends on Network Topology. Build Simul Rome 2019 2019:1–8.

[17] Schluck T, Kräuchi P, Sulzer M. Non-linear thermal networks - How can a meshed network improve energy efficiency? CISBAT, 09 - 11 Sept. 2015, Lausanne, Lausanne: 2015. doi:10.5075/epfl-cisbat2015-779-784.

[18] ETHZ. Die Energie von morgen, Energiekonzept Anergienetz ETH Hönggerberg. ETH Zurich, Abteilung Immobilien; 2017.

[19] Vetterli N, Thaler E, Sulzer M, Ryser P. Monitoring Suurstoffi, Schlussbericht. Bern: Bundesamt für Energie BFE; 2017.

[20] Prasanna A, Dorer V, Vetterli N. Optimisation of a district energy system with a low temperature network. Energy 2017;137:632–48. doi:10.1016/j.energy.2017.03.137.

[21] Rüsch F, Rommel M, Haller M. TARO-Thermische Arealvernetzung Energetische Optimierung anhand von dynamischen Systemsimulationen. Bern: Bundesamt für Energie BFE; 2016.

[22] Franzén I, Nedar L, Andersson M. Environmental Comparison of Energy Solutions for Heating and Cooling. Sustainability 2019;11:7051. doi:10.3390/su11247051.

[23] Wetter M, Hu J. Quayside Energy Systems Analysis. Lawrence Berkeley National Laboratory; 2019.

[24] Sommer T, Mennel S, Sulzer M. Lowering the pressure in district heating and cooling networks by alternating the connection of the expansion vessel. Energy 2019;172:991–6. doi:10.1016/j.energy.2019.02.010.

[25] Lennermo G, Lauenburg P, Brand L. Decentralized heat supply in district heating systems - implications of varying differential pressure. 14th Int Symp DH Cool 2014:6.

[26] Lennermo G, Lauenburg P, Werner S. Control of decentralised solar district heating. Sol Energy 2019;179:307–15. doi:10.1016/j.solener.2018.12.080.

[27] Sulzer M, Sotnikov A, Sommer T. Reservoir-Niedertemperatur Netztopologie für die Vermaschung von thermischen Netzen. brenet Conf. Proc., Zurich: BFE, Innosuisse; 2018, p. 590.

[28] Sommer T, Sotnikov A, Sandmeier E, Stettler C, Mennel S, Sulzer M. Optimization of low-temperature networks by new hydraulic concepts. J Phys Conf Ser 2019:1343. doi:10.1088/1742-6596/1343/1/012112.

[29] Wetter M, Zuo W, Nouidui TS, Pang X. Modelica Buildings library. J Build Perform Simul 2014;7:253–70. doi:10.1080/19401493.2013.765506.

[30] Gagné-Boisvert L, Bernier M. Integrated model for comparison of one- and two-pipe ground-coupled heat pump network configurations. Sci Technol Built Environ 2018;24:726–42. doi:10.1080/23744731.2017.1366184.

[31] Sotnikov A, Sandmeier E, Sulzer M, Sergi T, Mennel S, Sommer T. Thermal stability and heat transfer in the reservoir low temperature network. J Phys Conf Ser 2019:1343. doi:10.1088/1742-6596/1343/1/012113.

[32] Mattsson SE, Elmqvist H. Modelica - An International Effort to Design the Next Generation Modeling Language. IFAC Proc Vol 1997;30:151–5. doi:10.1016/s1474-6670(17)43628-7.

[33] Kauko H, Kvalsvik KH, Rohde D, Nord N, Utne Å. Dynamic modeling of local district heating grids with prosumers: A case study for Norway. Energy 2018;151:261–71. doi:10.1016/j.energy.2018.03.033.

[34] Schweiger G, Larsson PO, Magnusson F, Lauenburg P, Velut S. District heating and cooling systems – Framework for Modelica-based simulation and dynamic optimization. Energy

2017;137:566–78. doi:10.1016/j.energy.2017.05.115.

[35] Zarin Pass R, Wetter M, Piette MA. A thermodynamic analysis of a novel bidirectional district heating and cooling network. Energy 2018;144:20–30. doi:10.1016/j.energy.2017.11.122.

[36] Bünning F, Wetter M, Fuchs M, Müller D. Bidirectional low temperature district energy systems with agent-based control: Performance comparison and operation optimization. Appl Energy 2017:0–1. doi:10.1016/j.apenergy.2017.10.072.

[37] von Rhein J, Henze GP, Long N, Fu Y. Development of a topology analysis tool for fifth-generation district heating and cooling networks. Energy Convers Manag 2019;196:705–16. doi:10.1016/j.enconman.2019.05.066.

[38] Murray P, Niffeler M, Mavromatidis G, Orehounig K. Optimal retrofitting measures for residential buildings at large scale: a multi-objective approach. Int Build Simul Conf 2019, Rome, Italy 2019.

[39] Orehounig K, Sulzer M. Technische Regulierung im Gebäudebereich 2019. http://www.nfp70.ch/de/projekte/ergaenzungsstudien/technische-regulierung-im-gebaeudebereich.

[40] Murray P, Marquant J, Niffeler M, Mavromatidis G, Orehounig K. Optimal transformation strategies for buildings, neighbourhoods and districts to reach CO2 emission reduction targets. Energy Build 2020;207:109569. doi:10.1016/j.enbuild.2019.109569.

[41] SIA. SIA 2014:2015 Raumnutzungsdaten für die Energie- und Gebäudetechnik. Schweizerischer Ingenieur- und Architektenverein; 2015.

[42] Staub P, Rütter H. Die volkswirtschaftliche Bedeutung der Immobilienwirtschaft der Schweiz. Zürich: pom+, HEV Schweiz; 2014.

[43] BFS. Wohnfläche pro Bewohner: Der Systemwechsel von 2000 auf 2012, Gebäude- und Wohnungsstatistik (GWS),. Bundesamt für Statistik BFS; 2014.